Physica Scripta. Vol. 60, 90–96, 1999

Optical Constants in the Subgap Region and Vibrational Behaviour by Far-Infrared Spectroscopy of Wedge-Shaped Obliquely-Deposited Amorphous GeS_2 Films

E. Márquez,[1]* A. M. Bernal-Oliva,[1] J. M. González-Leal,[1] R. Prieto-Alcón[1], J. C. Navarro[1] and D. Minkov[2]

[1] Departamento de Física de la Materia Condensada, Facultad de Ciencias, Universidad de Cádiz, Apdo. 40, 11510-Puerto Real (Cádiz), Spain
[2] Research Institute for Fracture Technology, Tohoku University, Sendai, Japan

Received April 27, 1998; accepted in revised form December 7, 1998

PACS ref: 81.05.Gc; 81.15.Ef; 78.20.-e; 78.20.Ci; 63.50.+x

Abstract

Optical transmission spectra are very sensitive to inhomogeneities of thin films. In particular, non-uniform film thickness leads to shrinking of the transmission spectrum at normal incidence. This non-uniformity has to be taken into account, because its ignorance may lead to serious errors in the calculated values of the refractive index and the film thickness. This paper presents a method, which transforms the optical transmission spectrum of a wedge-shaped thin film into a spectrum of a uniform film whose thickness is equal to the average thickness of the non-uniform film. This allows to calculating the refractive index, the average thickness, as well as a parameter indicating the degree of film thickness uniformity. The method is successfully applied to wedge-shaped obliquely-deposited chalcogenide glass thin films of chemical composition GeS_2. The dispersion of the refractive index in the subgap region is discussed in terms of the Wemple-DiDomenico single-oscillator model. The optical-absorption edge is described using the 'non-direct transition' model suggested by Tauc, and the optical gap is calculated by Tauc's extrapolation. Far-infrared spectroscopy has been used to clearly complement the results derived from the present optical measurements.

1. Introduction

Over the last two decades, interest in the knowledge of the optical properties of chalcogenide glasses has grown considerably, owing to the wide range of phenomena exhibited by these semiconducting materials, when certain samples are exposed to light or other irradiation [1-3]. In general, these phenomena are accompanied by changes in the optical constants of the material and, in particular, shifts in the absorption edge, i.e., photo-darkening or photo-bleaching. The accurate determination of the optical constants of these glassy materials is a prerequisite, not only for complete understanding of the basic mechanisms of the photo-induced phenomena, but also for exploiting of their technological potential.

Existing methods for determination of the optical constants, based exclusively on the optical transmission spectra at normal incidence [4,5], have already been applied to different crystalline and amorphous thin films, deposited on transparent substrates [6-8]. These relatively simple methods, are fairly accurate, being also non-destructive, and not requiring any previous knowledge of the thickness of the deposited film, while the thickness and the refractive index would be determined within an error of about 2% [5]. They do, however, assume a uniform thickness of the film, while the use of non-uniform films results in shrinking of the optical transmission spectrum, leading to less accurate calculated results and even serious errors.

* e-mail address: emilio.marquez@uca.es

In the present paper, a physically appealing procedure for optical characterisation of non-uniform thin films, suggested by Swanepoel [9], has been employed. The method uses a transformation of the transmission spectrum corresponding to a film of non-uniform thickness to a spectrum of a uniform film, whose thickness is equal to the average thickness of the non-uniform film. The method is applied to calculating of the geometrical parameters, average thickness and the thickness variation, and the refractive index in the subband-gap region of thermally-evaporated wedge-shaped glass films, obliquely deposited, of chemical composition, GeS_2 (i.e., germanium sulphide). The results obtained for three representative thin-film samples, designated as F1, F2 and F3, are presented in this work. Furthermore, far-infrared spectroscopy is used to obtain a very useful structural information (i.e., the vibrational behaviour of the amorphous solid) that strongly complements the results obtained from the present optical measurements.

2. Experimental details

Thin-film samples were prepared by vacuum evaporation of powdered melt-quenched glassy material (made by heating of an appropriate mixture of the elements in vacuum-sealed fused-silica ampoules, for about 4 h, at approximately 900 °C, and air-quenched) onto clean glass substrates (BDH Superpremium) and Si wafer substrates. The thermal evaporation process was carried out in a coating system (Edwards, model E306A), at a pressure of $\approx 5 \times 10^{-7}$ Torr, from a suitable quartz crucible. The samples were deposited obliquely at various angles of incidence (20°-40°). The temperature rise of the substrate, due to radiant heating from the crucible, was negligible during the deposition process. The deposition rate was ≈ 0.4 nms^{-1}, which was measured continuously by a quartz-crystal monitor (Edwards, model FTM-5). It is known that such a low deposition rate produces a film composition which is very close to that of the bulk starting material, while electron microprobe analysis indicated that the film stoichiometry is correct within ±1 at. %. Care was taken to minimize exposure to light sources during sample preparation, and the thin-film samples were kept in complete darkness until their use. These measures were taken to diminish the photo-bleaching, which is a light-induced effect that occurs in Ge-based chalcogenide glasses [10], and results in a significant decrease of the refractive index.

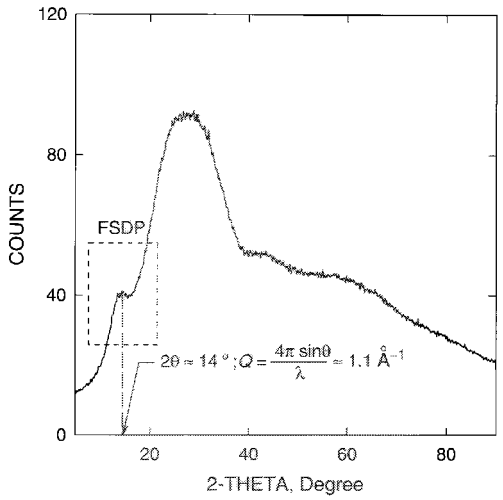

Fig. 1. X-ray diffraction pattern (Cu Kα radiation) of a representative as-evaporated germanium sulphide glass film (the data have been smoothed by means of the Savitzky-Golay filter).

The lack of crystallinity in the film was verified by X-ray diffraction (XRD) analysis. Figure 1 shows a typical XRD-pattern, using the Cu Kα line, for as-deposited germanium sulphide films. The first sharp diffraction peak (FSDP), which is observed at an angle of $2\theta \approx 14°$, is associated with the medium-range order of the amorphous structure [11,12].

The optical transmission spectra were obtained over the spectral region 400-2500 nm by a double-beam, UV/Vis/NIR computer-controlled spectrophotometer (Perkin-Elmer, model Lambda-19). The area of illumination over which the transmission spectra were obtained, was approximately 1×10 mm^2. It should be emphasized that the transmission spectra show unambiguously that the α-GeS_2 films have non-uniform thickness. This was confirmed by mechanical measurements of the film thickness, using a stylus-based surface profilometer (Sloan, model Dektak 3030). The IR-transmission spectra were obtained in the 800-30 cm^{-1} range by a computer-controlled FTIR spectrometer (Perkin-Elmer, model 2000). All optical and IR measurements reported in this paper were made at room temperature. Finally, the film thickness studied was in the range of approximately 1000-2200 nm.

3. Derivation of analytical expressions for the envelopes of the transmission spectra of non-uniform films

A thin homogeneous film with uniform thickness, d, and complex refractive index, $n_c = n - ik$, and absorption coefficient, α, is considered initially. The film is deposited on a transparent substrate with refractive index, s. This system is surrounded by air with refractive index $n_0 = 1$. The expression for the transmittance, T, at normal incidence is [5,9,13]:

$$T = \frac{Ax}{B - Cx\cos\varphi + Dx^2}, \tag{1}$$

while all multiple reflections are taken into account, and, on the otherhand, $k^2 \ll n^2$, $A = 16\,n^2 s$, $B = (n+1)^3(n+s^2)$, $C = 2(n^2-1)(n^2-s^2)$, $D = (n-1)^3(n-s^2)$, $\varphi = 4\pi nd/\lambda$, $x = \exp(-\alpha d)$ and, finally, $k = \alpha\lambda/4\pi$. The envelopes around the interference maxima, T_{M0}, and minima, T_{m0}, are continuous functions of λ, and:

$$T_{M0} = \frac{Ax}{B - Cx + Dx^2}, \tag{2a}$$

$$T_{m0} = \frac{Ax}{B + Cx + Dx^2}. \tag{2b}$$

The case considered in this paper is illustrated schematically in Fig. 2. It is assumed that the thickness of the film varies linearly over the illuminated area, and can be expressed as: $d = \bar{d} \pm \Delta d$. Δd is the linear variation of the thickness around the average thickness $\bar{d}$ as shown in Fig. 2, and Δd is not the standard deviation of calculated values or the r.m.s. deviation used elsewhere [14]. The transmittance measurements are performed in such a way that the same area is illuminated for all wavelengths.

The theory developed in this paper refers to a linear variation of d over a macroscopic scale of typically a few millimetres; it is, however, also valid in the cases of triangular, rectangular and sinusoidal surface roughness. The effect of thickness variation on a typical transmission spectrum is shown in Fig. 3. It is seen that the interference pattern shrinks notably if the thickness is not uniform. This effect is further investigated next.

For non-uniform films the transmittance, T, at a specific wavelength, λ, can be obtained by integrating Eq. (1) over both Δd and x. This is prohibitively difficult analytically, and an approximation is to use the average value of x, $\bar{x} = \exp(-\alpha\bar{d})$ over the integration range Δd. This approximation is precise provided that $\Delta d \ll \bar{d}$. Correspondingly the expression for the transmittance T becomes [9]:

$$T = \frac{1}{\varphi_2 - \varphi_1}\int_{\varphi_1}^{\varphi_2} \frac{A\bar{x}}{B - C\bar{x}\cos\varphi + D\bar{x}^2}\,d\varphi, \tag{3}$$

where $\varphi_1 = 4\pi n(\bar{d} - \Delta d)/\lambda$ and $\varphi_2 = 4\pi n(\bar{d} + \Delta d)/\lambda$. The

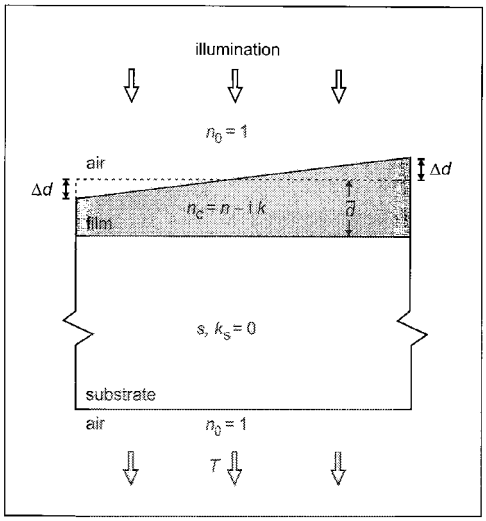

Fig. 2. Schematic drawing of a weakly absorbing thin film with a linear variation in thickness on a thick transparent substrate.

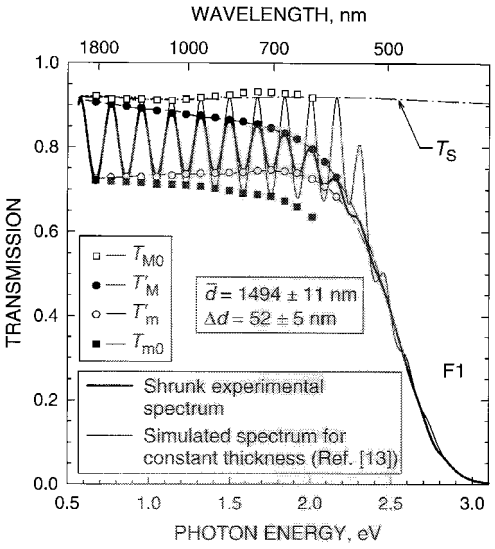

Fig. 3. Transmission spectrum of a representative wedge-shaped thin film of GeS_2 chalcogenide glass, deposited onto thick transparent substrate. The average thickness of this sample is 1494 ± 11 nm. T'_M, T'_m, T_{M0} and T_{m0} are introduced in the text and T_s is the transmission of the substrate alone.

integral solution gives [9]:

$$T = \frac{\lambda}{4\pi n\Delta d}\frac{a}{(1-b^2)^{1/2}} \left[\tan^{-1}\left(\frac{1+b}{(1-b^2)^{1/2}}\tan\frac{\varphi_2}{2}\right) - \tan^{-1}\left(\frac{1+b}{(1-b^2)^{1/2}}\tan\frac{\varphi_1}{2}\right)\right], \tag{4}$$

where

$$a = \frac{A\bar{x}}{B + D\bar{x}^2}, \tag{4a}$$

and

$$b = \frac{C\bar{x}}{B + D\bar{x}^2}. \tag{4b}$$

Furthermore, the expressions for the envelopes around the interference maxima and minima of the transmission spectrum are [9]:

$$T_M = \frac{\lambda}{2\pi n\Delta d}\frac{a}{(1-b^2)^{1/2}}\tan^{-1}\left[\frac{1+b}{(1-b^2)^{1/2}}\tan\left(\frac{2\pi n\Delta d}{\lambda}\right)\right], \tag{5}$$

$$T_m = \frac{\lambda}{2\pi n\Delta d}\frac{a}{(1-b^2)^{1/2}}\tan^{-1}\left[\frac{1-b}{(1-b^2)^{1/2}}\tan\left(\frac{2\pi n\Delta d}{\lambda}\right)\right]. \tag{6}$$

The substitution of Eqs. (4a) and (4b) into Eqs. (5) and (6), and the use of Eqs. (2a) and (2b) gives the following expressions for the experimental envelopes, T'_M and T'_m, of the non-uniform film as functions of the envelopes T_{M0} and T_{m0} of the corresponding uniform film, with a thickness equal to the average thickness of the non-uniform film:

$$T'_M = \frac{(T_{M0}T_{m0})^{1/2}}{\chi}\tan^{-1}\left[\left(\frac{T_{M0}}{T_{m0}}\right)^{1/2}\tan\chi\right], \tag{7}$$

$$T'_m = \frac{(T_{M0}T_{m0})^{1/2}}{\chi}\tan^{-1}\left[\left(\frac{T_{m0}}{T_{M0}}\right)^{1/2}\tan\chi\right], \tag{8}$$

where:

$$\chi = 2\pi n\Delta d/\lambda, \tag{9}$$

and

$$0 < \chi < \pi/2 \text{ (or equivalently, } 0 < \Delta d < \lambda/4n). \tag{10}$$

4. Calculation of T_{M0} and T_{m0}

4.1. *Theoretical considerations for calculation of* T_{M0} *and* T_{m0}

Equations (7) and (8) are two independent transcendental equations for T_{M0}, T_{m0} and χ. In the transparent region, $T_{M0} \equiv T_s$ (see Fig. 3), and Eqs. (7) and (8) can be solved for T_{m0} and χ in this spectral region, using a rapidly converging algorithm (Newton-Raphson iteration). In this transparent region, n is determined from the following expression:

$$T_{m0} = \frac{4n^2 s}{n^4 + n^2(s^2+1) + s^2}. \tag{11}$$

Δd can be obtained from Eq. (9), but a more useful procedure in most cases, from the standpoint of unambiguously evaluating the uniformity parameter Δd, will now be presented.

It was shown in previous works [5,9] that the equation for the order numbers of the extrema of the interference fringes is:

$$\frac{\ell}{2} = \frac{2n\bar{d}}{\lambda} - m_1 \qquad \ell = 0, 1, 2, 3, \ldots \tag{12}$$

for the successive extrema, starting from the long-wavelength end, where m_1 is the order number of the first ($\ell = 0$) extremum considered, and while m_1 is an integer for a maximum or a half-integer for a minimum. The substitution of Eq. (9) in Eq. (12) gives:

$$\frac{\ell}{2} = \left(\frac{\bar{d}}{\pi\Delta d}\right)\chi - m_1. \tag{13}$$

A plot of $\ell/2$ as a function of χ in the transparent region allows to determining the slope and m_1, based on Eq. (13), which is illustrated in Fig. 4. Equation (13) can be used next for calculation of χ for the extrema in the absorption region, and T_{M0} and T_{m0} can be calculated then from Eqs. (7) and (8), as discussed below in detail.

4.2. *An example of calculation of* T_{M0} *and* T_{m0}

The experimental transmission spectrum shown in Fig. 3, corresponds to the representative wedge-shaped thin-film sample F1. The transmission of the substrate alone is also included as T_s. The envelopes, T'_M and T'_m, are drawn around the extrema

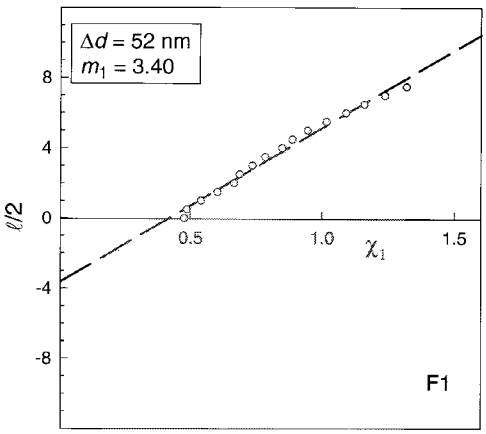

Fig. 4. Plot of $\ell/2$ as a function of χ_1 in order to determine m_1 for the representative GeS_2 film, F1.

of each transmission spectrum and the values obtained from these envelopes are used in the following calculations. It is noteworthy to mention that the iterative method for determining the envelope curves of a given set of oscillatory data, proposed by McClain *et al.* [15], was used for obtaining of the envelope functions in numerical form. The results of the calculations for the transmission spectrum from Fig. 3 are given in Table I as a representative example.

T_{m0} and χ are calculated initially from Eqs. (7) and (8), using the values of T'_M and T'_m for the extrema listed in Table I, and substituting $T_{M0}(\lambda) = T_s(\lambda)$. The values of χ are shown as χ_1 in Table I. Fig. 4 shows the plot of $\ell/2$ as a function of χ_1 according to Eq. (13), while the best straight line fit for the points of the transparent region is also drawn. The points for larger χ_1, which deviate from this straight line, indicate the onset of absorption and these points have to be ignored when the straight line is drawn. The following expression:

$$\ell/2 = 8.43\chi - 3.40, \tag{13a}$$

is correspondingly obtained for the representative thin-film sample F1, based on Fig. 4 and Eq. (13).

The value of χ at each extremum is calculated using a new expression derived by modifying the above equation, in such a way that the value of m_1 is appropriately rounded. The new values of χ are also included in Table I. T_{M0} and T_{m0} are calculated from Eqs. (7) and (8), using these values of χ and T'_M and T'_m. The values of T_{M0} and T_{m0} are also included in Table I.

The calculated values of T_{M0} and T_{m0} are finally used to calculate $\bar{d}$, Δd, $n(\lambda)$, $\alpha(\lambda)$ and $k(\lambda)$, using the method for uniform films, discussed in detail in [5,8,16]. A brief discussion of this method follows.

5. Calculation of $\bar{d}$, Δd, $n(\lambda)$, $\alpha(\lambda)$ and $k(\lambda)$

The essence of the calculation procedure is the determination of the exact order numbers of the extrema of the transmission spectrum, and the accurate calculation of the thickness of the layer, based on approximate values of the refractive index, n_1, and the thickness of the layer, d_1. The expression for n_1 is:

$$n_1 = [N + (N^2 - s^2)^{1/2}]^{1/2}, \tag{14}$$

where

$$N = 2s\frac{T_{M0} - T_{m0}}{T_{M0}T_{m0}} + \frac{s^2 + 1}{2}.$$

The refractive index of the substrate at each wavelength is derived from $T_s(\lambda)$, using the well-known equation:

$$s = \frac{1}{T_s} + \left(\frac{1}{T_s^2} - 1\right)^{1/2}. \tag{15}$$

Moreover, the first approximate value of the layer thickness is given by the expression:

$$d_1 = \frac{\lambda_1\lambda_2}{2(n_{e2}\lambda_1 - n_{e1}\lambda_2}, \tag{16}$$

Table I. *Values of λ, T'_M and T'_m for the typical optical transmission spectrum of the representative thin-film sample, F1. The underlined transmittance values are those calculated by the iterative method proposed by McClain* et al. *[15] (see Fig. 3). T_{M0} and T_{m0} were calculated from T'_M and T'_m and the envelope method for uniform films was used next. It is worth noting that the exact values of m_1 derived from Eq. (13) are usually the same as the values obtained from the procedure for uniform films.*

Sample	λ (nm)	s	T'_M	T'_m	χ_1	χ	T_{M0}	T_{m0}	n_1	d_1 (nm)	m_0	m	d_2 (nm)	n_2
F1	1847	1.513	0.908	0.725	0.48	0.40	0.921	0.721	2.141	—	3.27	3.5	1510	2.140
	1621	1.513	0.902	0.728	0.49	0.46	0.914	0.720	2.140	—	3.72	4.0	1515	2.145
	1444	1.529	0.898	0.729	0.54	0.52	0.914	0.718	2.160	1475	4.22	4.5	1504	2.149
	1305	1.529	0.893	0.729	0.60	0.58	0.914	0.715	2.168	1464	4.68	5.0	1505	2.158
	1185	1.535	0.887	0.730	0.67	0.64	0.912	0.713	2.178	1457	5.18	5.5	1496	2.156
	1088	1.535	0.881	0.733	0.69	0.70	0.911	0.712	2.179	1466	5.64	6.0	1498	2.159
	1011	1.543	0.878	0.736	0.73	0.76	0.915	0.711	2.195	1503	6.12	6.5	1497	2.174
	941	1.533	0.876	0.737	0.78	0.82	0.919	0.707	2.204	1469	6.60	7.0	1494	2.179
	881	1.531	0.871	0.739	0.85	0.88	0.922	0.703	2.220	1433	7.10	7.5	1488	2.186
	829	1.517	0.866	0.739	0.89	0.94	0.925	0.698	2.230	1441	7.58	8.0	1487	2.193
	784	1.518	0.861	0.741	0.94	1.00	0.930	0.692	2.236	1390	8.04	8.5	1490	2.204
	742	1.515	0.855	0.745	1.02	1.06	0.933	0.689	2.256	1362	8.57	9.0	1480	2.209
	707	1.512	0.846	0.747	1.09	1.12	0.932	0.684	2.278	1461	9.08	9.5	1474	2.221
	674	1.511	0.834	0.744	1.16	1.17	0.929	0.674	2.269	1367	9.49	10.0	1485	2.229
	647	1.510	0.820	0.739	1.24	1.23	0.927	0.660	2.274	1238	9.90	10.5	1494	2.247
	617	1.509	0.797	0.726	1.32	1.29	0.918	0.635	2.285	1200	10.40	11.0	1485	2.255

$\bar{d}_1 = 1409 \pm 90$ nm (6.4%); $\bar{d}_2 = 1494 \pm 11$ nm (0.7%)

where n_{e1} and n_{e2} are the refractive indices for two adjacent maxima (or minima) at λ_1 and λ_2. On the other hand, the 'order number' of a given extremum, m_0, is estimated from the basic equation for interference fringes, $2nd = m\lambda$, using the average value of $d_1, \bar{d}_1$, and the corresponding n_1. The orders m of the neighbouring extrema are, in fact, consecutive integers for the maxima and half-integers for the minima - the m-values are obtained by appropriately rounding of the m_0-values. The calculation of the next thickness approximation, d_2, is carried out via the interference condition, while n_1 and m are now used. The average value of d_2, $\bar{d}_2$, represents the final calculated thickness of the layer. Next, substituting $\bar{d}_2$ and m again into the interference condition, the final calculated refractive index, n_2, is obtained for each extremum.

The calculation of the average thickness and refractive index corresponding to the typical transmission spectrum of the thin-film sample F1, using the envelope method for uniform films, is clearly illustrated in Table I. On the other hand, the values of $\bar{d}_2$ for F1, F2 and F3 are 1494 ± 11 nm, 1663 ± 3 nm, 1794 ± 15 nm, respectively. The corresponding errors of these final values of the average thickness are 0.9%, 0.3% and 0.7%, respectively. In addition, the substitution of the values of $\bar{d}_2$ into Eq. (13) gives the values for Δd listed in Table II. It is generally observed that the larger average thickness leads to larger thickness variation. Alternatively, the film thicknesses were measured directly by the already mentioned Dektak 3030 mechanical profilometer. These measured values are usually very close, indeed, to those calculated by the present envelope-curve procedure. The differences between the directly measured values of the thickness, d_m, and the corresponding calculated values, $\bar{d}$, are +1.4%, +0.8% and −1.6% for the samples F1, F2 and F3, respectively (see Table II). The final values of the refractive index for the three amorphous germanium sulphide films are shown in Fig. 5, as a function of the wavelength.

Concerning to the procedure for the determination of the absorption and extinction coefficients, Swanepoel [5] recommends that, in the case of uniform films, the T_{M0}-curve has to be used over the whole range of the spectrum, namely in the regions of strong, medium and weak absorption. The derivation of absorbance, x, in the strong-absorption region is based on the expression for the optical dispersion that will be presented later. The corresponding expression for calculation of x is:

$$x = \frac{E_{M0} - \left[E_{M0}^2 - (n^2-1)^3(n^2-s^4)\right]^{1/2}}{(n-1)^3(n-s^2)}, \tag{17}$$

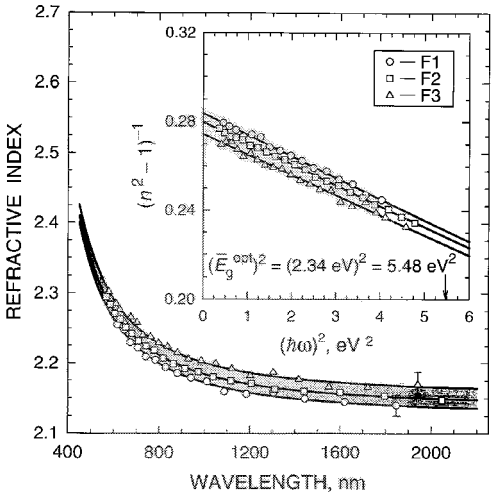

Fig. 5. Refractive index vs. wavelength for the as-deposited a-GeS_2 films, F1, F2 and F3. The inset is a plot of $(n^2-1)^{-1}$ vs. $(\hbar\omega)^2$ in the subband-gap region (the average value of the Tauc gap, $\bar{E}_g^{opt}$, is 2.34 ± 0.01 eV).

where

$$E_{M0} = \frac{8n^2 s}{T_{M0}} + (n^2-1)(n^2-s^2).$$

The absorption coefficient, $\alpha(\lambda)$, is then calculated, using the expression $\alpha = -(1/\bar{d})\ln x$. Once $\alpha(\lambda)$ is known, $k(\lambda)$ can be easily determined from the above-mentioned expression, $k = \alpha\lambda/4\pi$, which completes the derivation of the optical constants. The optical-absorption spectrum obtained by using Eq. (17) is displayed in Fig. 6, for the representative thin-film sample F1.

The optical band gap is derived from the obtained values of α. The absorption coefficient of amorphous semiconductors in the high-absorption region (where $\alpha \gtrsim 10^4$ cm^{-1}) is given, according to the 'non-direct transition' model suggested by Tauc [17], by the following relationship:

$$\alpha(\hbar\omega) = \frac{B\left(\hbar\omega - E_g^{opt}\right)^2}{\hbar\omega}, \tag{18}$$

where E_g^{opt} is the Tauc gap and $B^{1/2}$ is the Tauc slope. Such spectral dependence of the absorption coefficient can be associated to interband electronic transitions, and, in this case:

$$\alpha(\hbar\omega) \approx \frac{M}{\hbar\omega}\int_0^{\hbar\omega} g_v(-E)g_c(\hbar\omega - E)\mathrm{d}E, \tag{19}$$

where M is the transition matrix element, and g_v and g_c are the densities of states in the valence and conduction bands

Table II. *Thickness variation,* Δd, *film thickness measured by the stylus-based surface profiler,* d_m *average thickness,* $\bar{d}$, *Wemple-DiDomenico dispersion parameters,* E_0 *and* E_d, *Tauc gap,* E_g^{opt}, *gap ratio,* E_0/E_g^{opt}, *Ge coordination number,* N_c *and refractive index extrapolated at* $\hbar\omega = 0$, n(0), *for the three specimens F1, F2 and F3.*

Sample	Δd (nm)	d_m (nm)	$\bar{d}$ (nm)	E_0 (eV)	E_d (eV)	E_g^{opt} (eV)	E_0/E_g^{opt}	N_c	$n(0)$
F1	52 ± 5	1514 ± 30	1494 ± 11	5.47 ± 0.05	19.92 ± 0.20	2.36 ± 0.01	2.31 ± 0.03	3.2 ± 0.3	2.154 ± 0.001
F2	57 ± 3	1676 ± 34	1663 ± 3	5.44 ± 0.02	19.45 ± 0.07	2.32 ± 0.01	2.34 ± 0.02	3.3 ± 0.4	2.139 ± 0.001
F3	61 ± 7	1765 ± 35	1794 ± 15	5.45 ± 0.07	19.76 ± 0.30	2.35 ± 0.01	2.32 ± 0.04	3.4 ± 0.4	2.151 ± 0.002

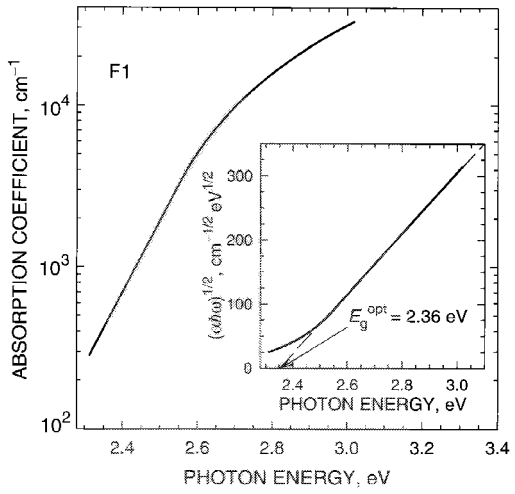

Fig. 6. Optical-absorption edge for the representative sample, F1, and, in the inset, the corresponding Tauc's extrapolation for determination of the optical gap.

of the amorphous semiconducting material. Assuming that these densities of states are parabolic functions, that is, $g_v(-E) \approx E^{1/2}$ and $g_c(E) \approx (E - E_g^{opt})^{1/2}$, and M is constant in the energy range under study, Eq. (19) takes on the form expressed by Eq. (18). Additionally, the Tauc gap can be determined by extrapolating $(\alpha\hbar\omega)^{1/2}$ towards zero (see the inset in Fig. 6). The values obtained for the optical gap for F1, F2 and F3 thin-film samples, are presented in Table II. These values are in very good agreement with those reported by other authors for thin films of the same glassy composition [18,19]. It should be mentioned that the band gap in the films is always lower than that of the bulk material (3.15 eV) [2].

6. Analysis of the optical dispersion based on the Wemple-DiDomenico single-oscillator framework

The refractive-index dispersion, $n(\omega)$, of crystalline and amorphous materials can be fitted by the Wemple-DiDomenico single-oscillator relation [20,21]:

$$\varepsilon_1(\omega) - 1 = n^2(\omega) - 1 = \frac{E_d E_0}{E_0^2 - (\hbar\omega)^2}, \tag{20}$$

where E_0 and E_d are single-oscillator fitting constants which measure the oscillator energy and strength, respectively. By plotting $(n^2 - 1)^{-1}$ as a function of $(\hbar\omega)^2$ and fitting a straight line as shown in Fig. 5, E_0 and E_d can be determined directly from the slope, $(E_0\, E_d)^{-1}$, and the intercept, E_0/E_d, on the vertical axis, respectively. The oscillator energy, E_0, is an 'average' energy gap, and it scales with the Tauc gap, E_g^{opt}, while $E_0 \approx 2 \times E_g^{opt}$, as it was found by Tanaka [22] investigating well-annealed As-S glass films. Furthermore, E_d obeys a simple empirical relationship:

$$E_d = \beta N_c Z_a N_e \text{ (eV)}, \tag{21}$$

where $\beta = 0.37 \pm 0.04$ eV for covalent crystalline and amorphous materials ($\beta = 0.26 \pm 0.03$ eV for ionic materials), N_c is the coordination number of the cation nearest neighbour to the anion, Z_a is the formal chemical valency of the anion, and N_e is the total number of valence electrons (cores excluded) per anion. The average values of E_0 and E_d (obtained from the values belonging to the samples F1, F2 and F3) are: $\bar{E}_0 = 5.45$ eV and $\bar{E}_d = 19.51$ eV. Moreover, the consideration that for this particular chalcogenide glassy composition, $Z_a = 2$ and $N_e = (4 \times 1 + 6 \times 2)/2 = 8$, gives an average value of the coordination number of the cation, $\bar{N}_c \approx 3.3 \pm 0.4$ (see also Table II). The very striking fact that $\bar{N}_c$ has a lower value than the expected value for GeS_2 thin films ($N_c = 4$), could be explained considering, on the one hand, that a 'shadowing' effect of the material deposited on the substrate with respect to the incoming evaporated atoms, incident at an oblique angle, leads to the formation of a columnar-growth morphology. Consequently, the mass density and the corresponding dispersion energy decrease substantially [21]. On the other hand, according to Pauling's electronegativities, the ionicity of Ge-S bonds is approximately 12%, which would account for a lower value of beta. Additionally, in ionic materials the more pronounced s-p splitting leads to s-like bands well below p-like bands, thus decreasing N_e.

In addition, the values of the gap ratio, E_0/E_g^{opt}, for the thin-film samples F1, F2 and F3 are 2.31, 2.34 and 2.32, respectively. Therefore, the present values of the Wemple-DiDomenico dispersion parameter, E_0, are reasonably consistent with the aforementioned relationship, $E_0 \approx 2 \times E_g^{opt}$.

7. IR-transmission measurements

IR-transmission measurements of amorphous germanium sulphide films, deposited onto Si wafer substrates, are discussed in detail next. It has been reported that the infrared spectra of the corresponding bulk glass could be interpreted in terms of a structural model based on a chemically-ordered phase [23]. The element of local order is a tetrahedral arrangement of S atoms around a central Ge atom. According to this local order, the above-mentioned value of $N_c = 4$ would be obviously expected. The tetrahedra are connected into a network through the twofold coordinated S atoms. The existence of such amorphous structure is also confirmed by RDF studies [24]. For an isolated tetrahedral molecule, there are four vibrational modes to be considered, which can be estimated from the reported frequencies of molecules, with similar structure and mass ratio. In this way, the frequencies of a GeS_4-molecule were calculated from the reported Raman frequencies of the $GeCl_4$-molecule [25]. Using this particular approach, the dominant IR and Raman modes occur at different frequencies, v_3(F2) at 388 cm^{-1} and v_1(A1) at 342 cm^{-1}, corresponding to the asymmetric and symmetric stretching modes of the tetrahedral molecules, respectively. In addition to the two previous bond-stretching modes, an XY_4-molecule has also two others bond-bending modes, a v_2-mode of E symmetry, which is only Raman active, and a v_4-mode of F_2 symmetry, which is both IR and Raman active. The frequency of the v_4-mode of a GeS_4-molecule is calculated to 147 cm^{-1}.

The far-infrared spectrum of an amorphous germanium sulphide film, deposited on a silicon substrate, is presented in Fig. 7, and a schematic representation of the proposed local order in the α-GeS_2 thin film is also included. The main feature of the IR spectrum at ≈ 370 cm^{-1} is due to bond-stretching vibrations of GeS_4 molecular units, while the absorption band at ≈ 150 cm^{-1} is due to bond-bending modes. In addition, an absorption band at around 740

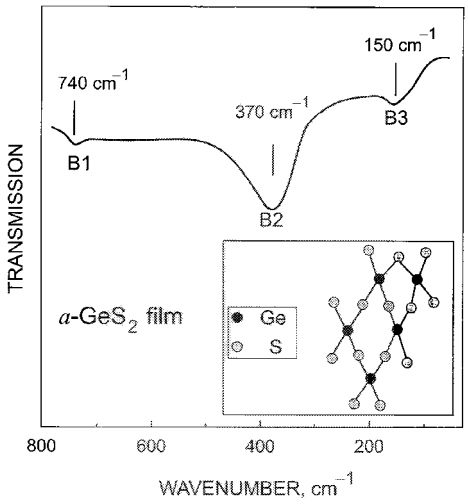

Fig. 7. IR-transmission spectrum of an amorphous germanium sulphide thin film, deposited onto a Si wafer substrate. The inset shows a schematic representation of the chemically-ordered network of four-coordinated Ge atoms and two-coordinated S atoms.

cm^{-1} could be associated with second-order processes (transverse optical modes $\approx 2 \times 370$ cm^{-1}).

8. Concluding remarks

The accurate method proposed in this paper for calculation of the geometrical parameters, average thickness and thickness variation, and the optical constants in the subgap region (0.5 - 2.3 eV) of wedge-shaped obliquely-evaporated amorphous germanium sulphide films, have been successfully applied to layers whose thickness ranges between approximately 1000 nm and 2200 nm. The lack of uniformity of the film thickness found under the present deposition conditions, leads to the strong shrinking of the interference fringes of the optical transmission spectrum at normal incidence. Consequently, inaccuracies and even very serious errors occur if $n(\omega)$, d and $\alpha(\omega)$ are calculated directly from such a shrunk transmission spectrum, assuming the layer to be uniform. Moreover, the simulated transmission spectrum corresponding to the case of a layer with constant thickness equal to the average thickness and with the same optical constants obtained for the thin-film sample F1 (see for all the corresponding details Ref. [13]), is also included in Fig. 3. The optical procedure used makes it possible to derive both the refractive index and the average thickness within an error of $\approx 1\%$. These results have been clearly corroborated by mechanical film thickness measurements, and also (and very significantly) using an independent optical characterization method for non-uniform thickness thin films, also proposed by Swanepoel [9,26]. The subsequent fitting of the obtained values of the refractive index to the Wemple-DiDomenico single-oscillator model, results in optical dispersion parameters directly related to the disordered structure of the chalcogenide material.

On the other hand, regarding the vibrational behaviour of the amorphous solid, we have presented the far-infrared spectrum of GeS_2 thin films and depicted a structural model based on a GeS_4-tetrahedrom. This model clearly explains the dominant features of the far-infrared spectrum which appears at ≈ 370 cm^{-1} (bond-stretching vibrations), at ≈ 150 cm^{-1} (bond-bending modes) and at ≈ 740 cm^{-1} (transverse optical modes).

Finally, several as-deposited amorphous germanium sulphide thin films were illuminated by a Hg arc lamp, through an IR-cut filter, with a light intensity of ≈ 30 $mWcm^{-2}$. As it has been previously reported [10], illumination of the present GeS_2 films produces a very strong blue shift of their optical transmission spectra. This indicates that a significant photo-bleaching process occurs in these particular Ge-based chalcogenide samples, which is in excellent agreement with the results obtained in [18,27,28]. Furthermore, the IR spectrum of the illuminated glass films shows vibrational bands at ≈ 670 cm^{-1} and at ≈ 825 cm^{-1}, due to the presence of Ge - O chemical bonds.

Acknowledgements

The authors are grateful to Prof. R. Swanepoel (Rand Afrikaans University, Johannesburg, South Africa), Dr. L. Tichý (Joint Laboratory, Pardubice, Czech Republic) and Dr. M. McClain (National Institute of Standards and Technology, Gaithersburg, USA) for fruitful discussions.

References

1. DeNeufville, J. P., in: "Optical Properties of Solids - recent developments", (ed. B. O. Seraphin), (North-Holland, Amsterdam, 1975).
2. Tanaka, Ka., J. Non-Cryst. Solids **35-36**, 1023 (1980).
3. Owen, A. E., Firth, A. P. and Ewen, P. J. S., Philos. Mag. B **52**, 347 (1985).
4. Manifacier, J. C., Gasiot J. and Fillard, J. P., J. Phys. E: Sci. Instrum. **9**, 1002 (1976).
5. Swanepoel, R., J. Phys. E: Sci. Instrum. **16**, 1214 (1983).
6. Hamman, M., Harith, M. A. and Osman, W. H., Solid State Commun. **59**, 271 (1986).
7. Kalomiros, J. A. and Spyridelis, J., Phys. Status Solidi (a) **107**, 633 (1988).
8. Márquez, E. *et al.*, J. Phys. D: Appl. Phys. **25**, 535 (1992).
9. Swanepoel, R., J. Phys. E: Sci. Instrum. **17**, 896 (1984).
10. Márquez, E., Bernal-Oliva, A. M., González-Leal, J. M., Prieto-Alcón, R. and Jiménez-Garay, R., J. Non-Cryst. Solids **222**, 250 (1997).
11. Luksha, O.V., Mikla, V. I., Ivanitsky, V. P., Mateleshko A.V. and Semak, D. G., J. Non-Cryst. Solids **144**, 253 (1992).
12. Elliott, S. R., J. Non-Cryst. Solids **106**, 26 (1988).
13. Heavens, O. S., "Optical Properties of Thin Solid Films", (Butterworths, London, 1955) p. 77.
14. Szczyrbowski, J. and Czapla, A., Thin Solid Films **46**, 127 (1977).
15. McClain, M., Feldman, A., Kahamer D. and Ying, X., Comput. Phys. **5**, 45 (1990).
16. Ramírez-Malo, J. B., Márquez, E., Villares P. and Jiménez-Garay, R., Mater. Lett. **17**, 327 (1993).
17. Tauc, J. J., Non-Cryst. Solids, **8-10**, 569 (1972).
18. Spence, C. A. and Elliott, S. R., Phys. Rev. B **39**, 5452 (1989).
19. Rajagopalan, S., Harshavardhan, K. S., Malhotra L. K. and Chopra, K. L., J. Non-Cryst. Solids **50**, 29 (1982).
20. Wemple, S. H. and DiDomenico, M., Phys. Rev. B **3**, 1338 (1971).
21. Wemple, S. H., Phys. Rev. B **7**, 3767 (1972).
22. Tanaka, Ke., Thin Solid Films **66**, 271 (1980).
23. Rowland, S. C., Narasimhan, S. and Bienenstock, A., J. Appl. Phys. **43**, 2741 (1972).
24. Cervinka, L. and Hruby, A., in "Proceedings of the Fifth International Conference on Liquid and Amorphous Semiconductors", (eds. J. Stuke and W. Brening), (Taylor and Francis, London, 1974) p. 431.
25. Lucovsky, G., Galeener, F. L., Keezer, R. C., Geits, R. H. and Six, K. A., Phys. Rev. B **10**, 5134 (1974).
26. González-Leal, J. M. *et al.*, Physica Scripta **55**, 108 (1997).
27. Tichý, L., Tichá, H. and Handlír, K., J. Non-Cryst. Solids **97-98** 1227, (1987).
28. Tichý, L., Tichá, H., Handlír K. and Jurek, K., J. Non-Cryst. Solids **101**, 223 (1988).